Poly(*m*-xylene adipamide)–Kaolinite and Poly(*m*-xylene adipamide)–Montmorillonite Nanocomposites

Anne Ammala, Anita J. Hill, Kelly A. Lawrence, Thuy Tran

CSIRO Manufacturing and Infrastructure Technology, Private Bag 33, South Clayton VIC 3169, Australia

Received 21 June 2005; accepted 5 July 2005
DOI 10.1002/app.22566
Published online in Wiley InterScience (www.interscience.wiley.com).

ABSTRACT: Two clay compounds, montmorillonite (Cloisite 30B) and kaolinite, were dispersed in a poly(*m*-xylene adipamide) resin at loading levels of 2 wt % clay. The samples were melt-compounded and extruded. The extruded samples were injection-molded into preforms and then blow-molded into multilayer bottles. Rheology, calorimetry, electron microscopy, and gas-transport measurements were performed. Both clays were nucleating agents, giving crystallite sizes that did not cause haze. Kaolinite was more difficult to exfoliate than montmorillonite, and under similar processing conditions, kaolinite resulted in a higher degree of crystallinity. Both nanocomposites exhibited improved gas-barrier properties over the neat resin. © 2007 Wiley Periodicals, Inc. J Appl Polym Sci 104: 1377–1381, 2007

Key words: barrier; crystallization; nanocomposites; nylon; organoclay

INTRODUCTION

Layered-silicate-based nanocomposites have received considerable attention in recent years as an effective method of enhancing polymer properties, such as increased stiffness and strength, improved gas-barrier properties, and superior flame retardancy.[1–4] The most preferred and widely used silicates are organically modified smectite clays with a 2 : 1-type layer structure such as montmorillonite.[5–8] These are commercially available from companies such as Southern Clay Products and Nanocor. Cloisite 30B, for example, is a montmorillonite clay treated with a hydroxyethyl quaternary cation and is compatible with polyamides such as nylon 6.

The most convenient way to produce these composites is melt compounding. A large number of polymer matrices have been used for the formation of nanocomposites by this technique.[9–11] This article focuses on a specific grade of nylon 6: poly(*m*-xylene adipamide) (MXD6).[12,13] MXD6 is finding increasing use in multilayer food packaging applications because of its inherent high oxygen-barrier properties and its rheology and processing conditions, which are comparable to those of poly(ethylene terephthalate) (PET) for use in, for example, carbonated beverage bottles.[14,15] Although the use of smectite clays with MXD6 has been previously reported to improve the gas barrier,[16] there is very little available data on the use of kaolinite with MXD6.

Unlike montmorillonite or other smectite clays, kaolinite is in a different group of clays and consists of a 1 : 1-type structure.[5–8] Although both kaolinite and montmorillonite possess a platelike structure and are capable of being exfoliated into the polymer matrix, they possess different cohesive energies between layers. In the 1 : 1 kaolinite structure, the layers are not charged, and interlayer bonding is due to hydrogen bonding via Al—OH groups on the inner surface. This strong hydrogen bonding makes delamination of kaolin more difficult than that for other platelike silicates such as montmorillonite, in which ions and water are present between the layers and interlayer bonding is weaker.

In this work, a chemical and mechanical pretreatment of kaolinite was used to facilitate exfoliation of the clay in the MXD6 matrix. There are very few literature reports on kaolinite nanocomposites in comparison with montmorillonite. Ethylene vinyl alcohol copolymer (EVOH)–kaolinite nanocomposites have been reported for potential applications in high-barrier food packaging,[17] and limited publications have been found for kaolinite–nylon 6 nanocomposites.[18] In this previously reported kaolinite–nylon 6 example, the resulting kaolinite nanocomposite was not exfoliated, and only the mechanical properties were investigated. The reported partially exfoliated EVOH–kaolinite nanocomposites were found to have increased the crystallinity and oxygen barrier. The purpose of this article is to examine the preparation of kaolinite–MXD6 and montmorillonite–MXD6 nanocomposites by melt processing and to exam-

Correspondence to: A. Ammala (anne.ammala@csiro.au).
Contract grant sponsor: ACI Plastics Packaging Australia.

Journal of Applied Polymer Science, Vol. 104, 1377–1381 (2007)

ine the degree of exfoliation, crystallinity, and gas-barrier properties of the resulting nanocomposite materials.

EXPERIMENTAL

Materials

MXD6 (6121; number-average molecular weight = 39,000) was acquired from Mitsubishi Gas Chemical Co. (Tokyo, Japan). Cloisite 30B (montmorillonite treated with a hydroxyethyl quaternary ammonium cation) was obtained from Southern Clay Products (Gonzales, TX) and was used as received. Kaolinite (Clay Q38) was obtained from Unimin Australia, Ltd (Sydney, Australia). To increase the degree of exfoliation of kaolinite in MXD6, it was chemically and mechanically pretreated through milling with a proprietary hyperdispersant based on carboxylic acid with ammonium functionality.

Melt compounding

Before the processing, MXD6 was dried *in vacuo* according to the manufacturer's instructions. Similarly, the cloisite and pretreated kaolinite were dried *in vacuo* before being blended with MXD6 pellets. The samples were prepared at a loading of 2 wt %.

Nanocomposite samples were obtained with a Theysohn corotating twin-screw extruder (length/diameter = 40) (Vienna, Australia). Various degrees of mixing were present along the length of the screws. Compounding was carried out at a barrel and die temperature of 262°C with a screw speed of 134 rpm. Extruded MXD6 nanocomposite pellets were dried *in vacuo* to remove moisture before being used as middle layers in coinjection-molded preforms and multilayer PET bottles. A neat sample of MXD6 (without clay additives) was extruded under identical conditions for comparison.

Rheology

Rheological measurements were performed at 246°C with a Monsanto capillary rheometer (St. Louis, MO) having a die diameter of 0.6375 mm and a length of 15.875 mm. The measurements were performed according to ASTM Standard D 3835.

Differential scanning calorimetry (DSC)

An analysis was performed with a Mettler–Toledo DSC 821[e] (Columbus, OH) under a nitrogen atmosphere with 8–10 mg for each run. Calibration of the DSC instrument was performed with a standard sample of indium. The same thermal history was given to all the samples and consisted of a first heating scan from room temperature to 300°C at a heating rate of 10°C/min. The samples were then held at 300°C for 10 min to ensure melting, and this was followed by a cooling scan to room temperature at 10°C/min. The samples were subsequently reheated to 300°C at 10°C/min, and the data were evaluated from the second heating step. The glass-transition temperature (T_g) was taken as the middle point of the specific heat incline in the glass-transition region. The crystallization temperature (T_c) and melting temperature (T_m) were taken as the maximum and minimum in the exothermic and endothermic peaks, respectively. The degree of crystallinity was determined from the DSC heat of fusion data and was defined as $(\Delta H_f/\Delta H_f^0) \times 100$, where ΔH_f is the experimental heat of fusion obtained by the integration of the heat flow and ΔH_f^0 is the heat of fusion for the purely crystalline form of the neat resin. For MXD6, the value of ΔH_f^0, taken from the manufacturer's published data, was 150.2 J/g.

Transmission electron microscopy (TEM)

TEM images of the nanocomposites were obtained at 100 kV with a Phillips EM 420 electron microscope (Eindhoven, Netherlands). The samples were ultramicrotomed with a diamond knife on a Reichert–Jung Ultracut E microtome (Wetzlar, Germany) at room temperature to give 60–80-nm-thick sections from a block of about 0.1 × 0.3 mm^2. The sections were collected on 200-mesh carbon-coated copper grids and subsequently dried with filter paper.

Haze

Sections of blow-molded bottles were cut from the center of each bottle, and the haze was measured with a Cary 1/3 spectrophotometer (Mulgrave, Australia) in accordance with the standard procedure (ASTM D 1003).

Carbon dioxide permeability

The carbon dioxide loss in the 390-mL blow-molded bottles was measured over 70 days with the standard procedure (ASTM F 1115). Data were collected periodically at 14-day intervals at 21.8 ± 0.4°C. Mean average results were taken over eight bottle samples.

RESULTS AND DISCUSSION

The haze values presented in Table I indicate that there is very little difference in the haze over the neat

TABLE I
Haze of the Multilayer Bottles

Bottle description	Haze (%)	Average section thickness (μm)
Neat MXD6	1.2	0.35
2 wt % cloisite	2.9	0.34
2 wt % kaolinite	4.3	0.37

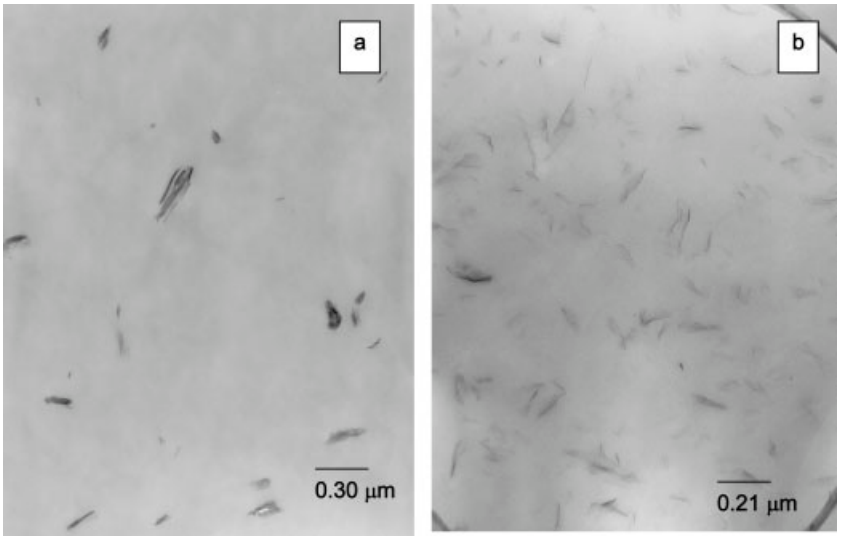

Figure 1 Low-resolution TEM micrographs of (a) the MXD6–kaolinite nanocomposite and (b) the MXD6–cloisite nanocomposite.

MXD6 resulting from the incorporation of nanoparticles. The clarity of the nanocomposites is very dependent on achieving a good dispersion of nanoparticles. In general, a haze value below 5% means that the substance is very transparent, and it is in the range required for most high-clarity packaging applications. Biaxially oriented PET typically has a haze value between 2 and 5%, and nylon has a value of typically 2–3%.[19] The haze data obtained from both the kaolinite and cloisite nanocomposites reveal that both materials are very suitable for applications requiring high clarity.

The clay dispersion and degree of exfoliation, examined by TEM, are compared for the extruded MXD6–kaolinite and MXD6–cloisite samples in Figure 1. Similarly, Figure 2 compares the samples at a higher resolution. It is apparent from both the low- and high-resolution images that the cloisite sample exhibits a higher degree of exfoliation than the kaolinite sample. The MXD6–kaolinite image reveals partial exfoliation with areas containing exfoliated platelets and areas of intercalated structures. The resulting kaolinite nanocomposite is reasonably intercalated even though the exfoliation of kaolinite is difficult because of the large cohesive energy between the layers. Figure 3 shows that some alignment of the clay platelets occurred after the extruded nanocomposites had undergone further injection molding and blow molding.

Figure 4 shows the rheological behavior of extruded nanocomposite samples versus the unextruded neat polymer. The behavior of the kaolinite sample closely followed that of the neat polymer, whereas that of the cloisite sample resulted in a slightly higher shear viscosity. Differences in the rheology due to the phase morphology (intercalated or exfoliated) of polymer layered-silicate nanocomposites have been reported

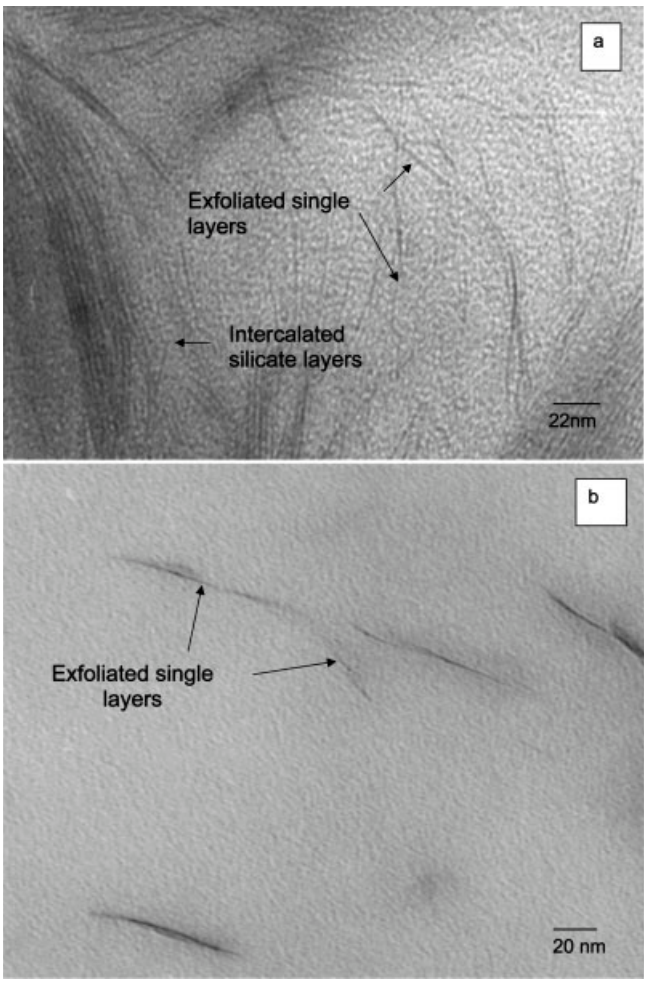

Figure 2 High-resolution TEM micrographs of (a) the MXD6–kaolinite nanocomposite and (b) the MXD6–cloisite nanocomposite.

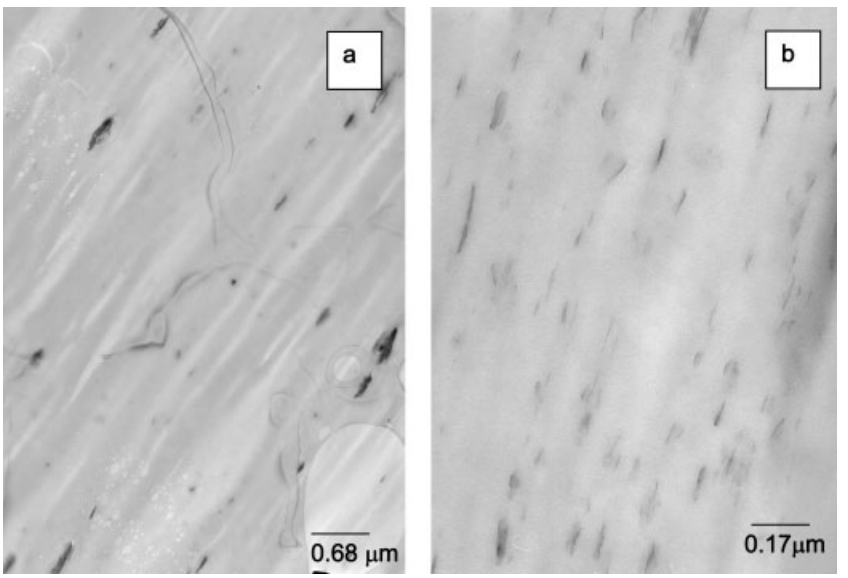

Figure 3 TEM micrographs of (a) the MXD6–kaolinite nanocomposite and (b) the MXD6–cloisite nanocomposite after blow molding.

previously.[20] In this case, the higher melt viscosity observed for cloisite over the kaolinite sample may be attributed to differences in the extent of exfoliation as observed by TEM.

Although it was not examined here, earlier experiments with a lower molecular weight MXD6 indicated a 30% reduction in the melt viscosity of the neat polymer after extrusion. This phenomenon has been reported elsewhere[21] and may be attributed to thermal degradation during melt blending. Similarly, the extruded neat MXD6 polymer used here is expected to have a lower melt viscosity than the unextruded neat resin.

A summary of the T_g, T_m, T_c, melting enthalpy (ΔH_f), and crystallinity (%) values, as determined by DSC, is presented in Table II. These parameters play an important role in determining polymer processability.

The DSC data show that T_g increases slightly in the nanocomposite samples versus neat MXD6. This can be attributed to a higher rigidity in the amorphous phase of the polymer in the presence of clay particles that restrict the molecular motions of the MXD6 chain segments. The magnitude of this increase is almost identical for both kaolinite and cloisite additives, with increases of 1.7 and 1.8°C, respectively.

T_m and ΔH_f also increase in the presence of nanoparticles. The magnitude of this change is higher for the kaolinite sample. Similarly, the kaolinite sample exhibited a higher degree of crystallinity and a higher T_c value than the cloisite sample. Increases of 12.7°C for T_c and 14.7% for the crystallinity were observed for kaolinite versus neat MXD6, whereas cloisite showed increases of 4.9°C for T_c and 7.0% for the crystallinity versus neat MXD6. This effect of increasing the crystallinity of MXD6 is very relevant for improved barrier applications because the crystalline regions are generally impermeable to the transport of gases and permeation is believed to occur through amorphous regions.

The increased crystallinity of the kaolinite nanocomposite can most likely be attributed to the effectiveness of kaolinite as a nucleating agent, which is reflected in the higher value of T_c. The kaolinite clay particles can act as seeds for spherulite growth in the molten nylon. The cloisite particles also act as nucleating agents; however, it appears that the kaolinite structure is more effective. As a result of this nucleating ability, the cooling time from the polymer melt can be reduced, and this is favorable during processing as it reduces the cycle time.

Gas permeability data for blow-molded multilayer PET–MXD6 bottles, shown in Figure 5, indicate that

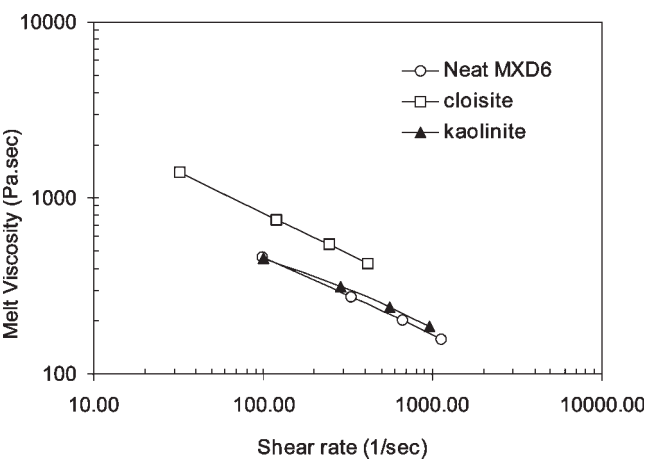

Figure 4 Melt viscosity versus the shear rate at 246°C for neat unextruded MXD6, the cloisite nanocomposite, and the kaolinite nanocomposite.

TABLE II
DSC Results for the Extruded Polymer Samples

Sample	T_g (°C)	T_m (°C)	T_c (°C)	ΔH_f (J/g)	Crystallinity (%)
Neat MXD6	86.7	236.2	180.7	53.1	35.4
MXD6 and 2% kaolinite	88.4	237.7	193.4	75.3	50.1
MXD6 and 2% cloisite	88.5	237.3	185.6	63.7	42.4

both MXD6–nanocomposite samples led to some improvement in the CO_2 barrier over the neat MXD6 polymer alone. After 14 days, the MXD6–kaolinite sample gave 7% higher retention of CO_2 than the neat MXD6, whereas the MXD6–cloisite sample gave a 4% improvement with respect to the neat resin. After 70 days, both MXD6–nanocomposite samples behaved similarly, with a 3% improvement in the CO_2 retention over neat MXD6.

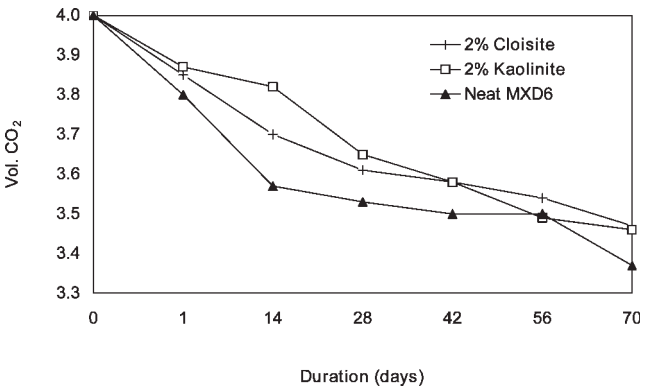

Figure 5 Carbonation retention data for blow-molded MXD6 and nanocomposite MXD6 bottles.

The mechanism in improving the gas barrier for MXD6 nanocomposites is dependent on several factors. Although good dispersion and exfoliation of clay platelets are highly desirable in increasing the tortuous path of gas molecules and maintaining good clarity, the effect of an additive on the polymer crystallinity seems equally important. The results obtained in this work clearly demonstrate that the MXD6–kaolinite nanocomposite is capable of giving the same level of improvement in the CO_2 gas barrier as the MXD6–cloisite nanocomposite, even though it is more difficult to exfoliate. These results make it clear that there is good potential for kaolinite nanocomposites to be used in high-barrier packaging applications.

CONCLUSIONS

MXD6–kaolinite and MXD6–cloisite nanocomposites were prepared by melt compounding. Both materials were easily processed with conventional equipment, and the resulting rheological and thermal properties indicated that preform and bottle blowing could be done with considerable ease. Investigations of the nanocomposite morphology, rheology, polymer crystallization behavior, haze, and CO_2 gas permeability were carried out. These studies showed that although the kaolinite nanocomposite was not as easily exfoliated as cloisite, similar levels of CO_2 permeability and haze were obtained. Kaolinite resulted in a larger increase in the MXD6 crystallinity than cloisite. Future studies will attempt to address the effect of the kaolinite loading as well as factors that improve the degree of exfoliation of kaolinite in nylon.

The authors thank ACI Plastics Packaging Australia for research funding and experimental assistance.

References

1. Alexandre, M.; Dubois, P. Mater Sci Eng 2000, 28, 1.
2. Schmidt, D.; Shah, D.; Giannelis, E. P. Curr Opin Solid State Mater Sci 2002, 6, 205.
3. Beyer, G. Plast Additives Compd 2002, 4, 22.
4. Ray, S. S.; Okamoto, M. Prog Polym Sci 2003, 28, 1539.
5. Theng, B. K. G. The Chemistry of Clay–Organic Reactions; Adam Hilger: London, 1974; p 1.
6. Theng, B. K. G. Formation and Properties of Clay–Polymer Complexes; Elsevier: Amsterdam, 1979; p 1.
7. Hall, P. L. A Handbook of Determinative Methods in Clay Mineralogy; Blackie: Glasgow, 1987; p 1.
8. Grim, R. E. Clay Mineralogy, 2nd ed.; McGraw-Hill: New York, 1968; p 57.
9. Liu, L.; Qi, Z.; Zhu, X. J Appl Polym Sci 1999, 71, 1133.
10. Vaia, R. A.; Ishii, H.; Giannelis, E. P. Chem Mater 1993, 5, 1694.
11. Christiani, B. R.; Maxfield, M. (to Allied Signal, Inc.). U.S. Pat. 5,747,560 (1998).
12. Lum, F. G. (to California Research Corp.). U.S. Pat. 2,997,463 (1961).
13. Miyamoto, A.; Shimizu, S.; Yamamiya, K.; Harada, M. (to Mitsubishi Gas Chemical Co., Inc.). U.S. Pat. 4,433,136 (1984).
14. d'Hount, J. P. (to Schmalbach–Lubeca PET Centre Technique et de Recherche SAS). Int. Pat. WO 98/58790 (1998).
15. Okudaira, T.; Tsuboi, A.; Sugihara, S.; Hama, Y. (to Toyo Boseki Kabushiki Kaisha). U.S. Pat. 4,398,642 (1983).
16. Lan, T.; Psihogios, V.; Bagrodia, S.; Germinario, L. T.; Gilmer, J. W. (to AMCOL International Corp.). U.S. Pat. 6,596,803 (2003).
17. Cabedo, L.; Gimenez, E.; Lagaron, J. M.; Gavara, R.; Saura, J. J Polymer 2004, 45, 5233.
18. Itagaki, T.; Matsumara, A.; Kato, M.; Usuki, A.; Kuroda, K. J Mater Sci Lett 2001, 20, 1483.
19. Leaversuch, R. Plast Technol 2002, 49, 48.
20. Lim, Y. T.; Park, O. O. Rheol Acta 2001, 40, 220.
21. Cho, J. W.; Paul, D. R. Polymer 2001, 42, 1083.